Electronic Supplementary Information

Flexible hierarchical membranes of WS_2 nanosheets grown on graphene-wrapped electrospun carbon nanofibers as advanced anodes for highly reversible lithium storage

Longsheng Zhang,[b] Wei Fan*[a] and Tianxi Liu*[a,b]

Fig. S1 FESEM image of the CNF membrane at low magnification, showing its three-dimensional nanofiber network with porous structures and large surface area.

Fig. S2 Cross-sectional FESEM images of the GCNF membrane at different magnifications. As indexed in (d), carbon nanofibers in the internal portion of GCNF membranes are wrapped by conductive graphene sheath.

Fig. S3 TEM images of GO sheets, showing that GO sheets are thin, a few microns in size and slightly scrolled on sheet edges.

Fig. S4 AFM image and the corresponding height profile of GO sheets, verifying that the thickness of single-layered GO sheets is about 1.0~1.1 nm.

Fig. S5 FESEM images of (a, c) WS_2/GCNF-1 and (b, d) WS_2/GCNF-3 hybrid membranes at low and high magnifications, respectively.

Fig. S6 TGA curves of WS_2, GCNF and WS_2/GCNF hybrid membranes.

Fig. S7 (a) Nitrogen adsorption/desorption isotherms of bare WS_2 powder and WS_2/GCNF-2 membrane. (b) The pore size distribution of WS_2/GCNF-2 membrane.

The WS_2 sample shows reversible type II isotherms while the WS_2/GCNF-2 sample exhibits type IV isotherms with a typical H2 hysteresis loop, indicating WS_2 powder as non-porous materials and WS_2/GCNF-2 membrane as mesoporous materials.

Fig. S8 Morphology of the WS_2/CNF hybrid membrane prepared *via* the same solvothermal method, without graphene sheath wrapping the carbon nanofibers. FESEM images of (a) WS_2/CNF-1, (b) WS_2/CNF-2 and (c) WS_2/CNF-3 hybrid membranes at low magnification. (d) FESEM image of WS_2/CNF-2 hybrid membrane at high magnification.

Fig. S9 FESEM images of the as-prepared WS_2 sample without adding CNF or GCNF membranes.

Fig. S10 High resolution C 1s spectra of (a) WS_2/GCNF-2 hybrid membrane and (b) GO sheets, confirming that most of the oxygen-containing functional groups (-C-O and -C=O groups) of the graphene sheets in WS_2/GCNF-2 hybrid membrane are removed after the thermal reduction process.

Fig. S11 Comparison of the electrochemical performance of WS_2/GCNF-1, WS_2/GCNF-2 and WS_2/GCNF-3 anodes at constant current density of 0.1 A g^{-1}.

Fig. S12 Cycling performance of CNF, WS_2/CNF-1, WS_2/CNF-2 and WS_2/CNF-3 anodes at constant current density of 0.1 A g^{-1}.

Fig. S13 Columbic efficiency of the WS_2/GCNF-2 hybrid membrane during the galvanostatic discharge-charge process.

Fig. S14 The post-mortem FESEM images of WS_2/GCNF-2 hybrid membrane after 100 cycles of discharge-charge tests.

Fig. S15 Nyquist plots of the WS_2 and WS_2/GCNF-2 electrode after 10 cycles.

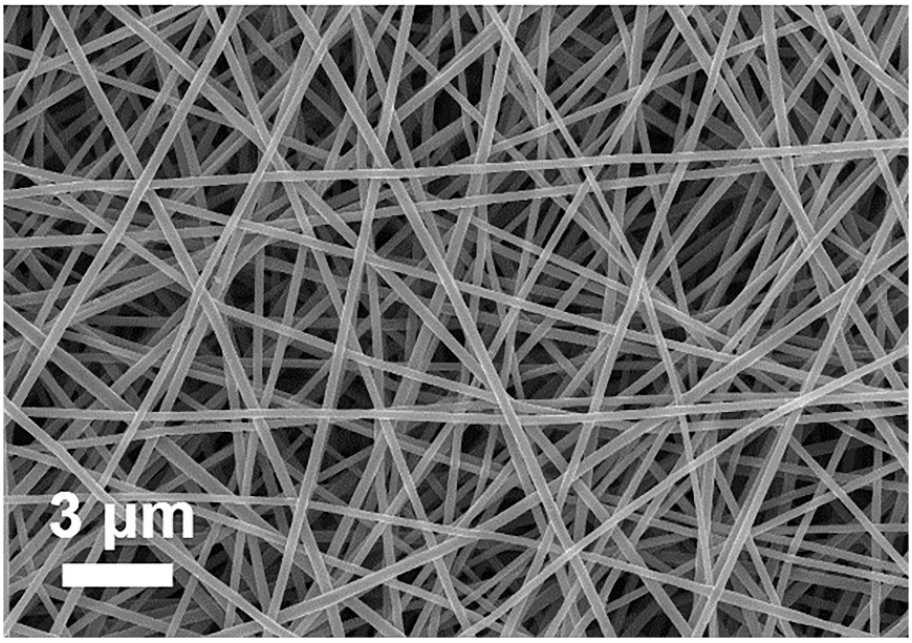

Fig. S1

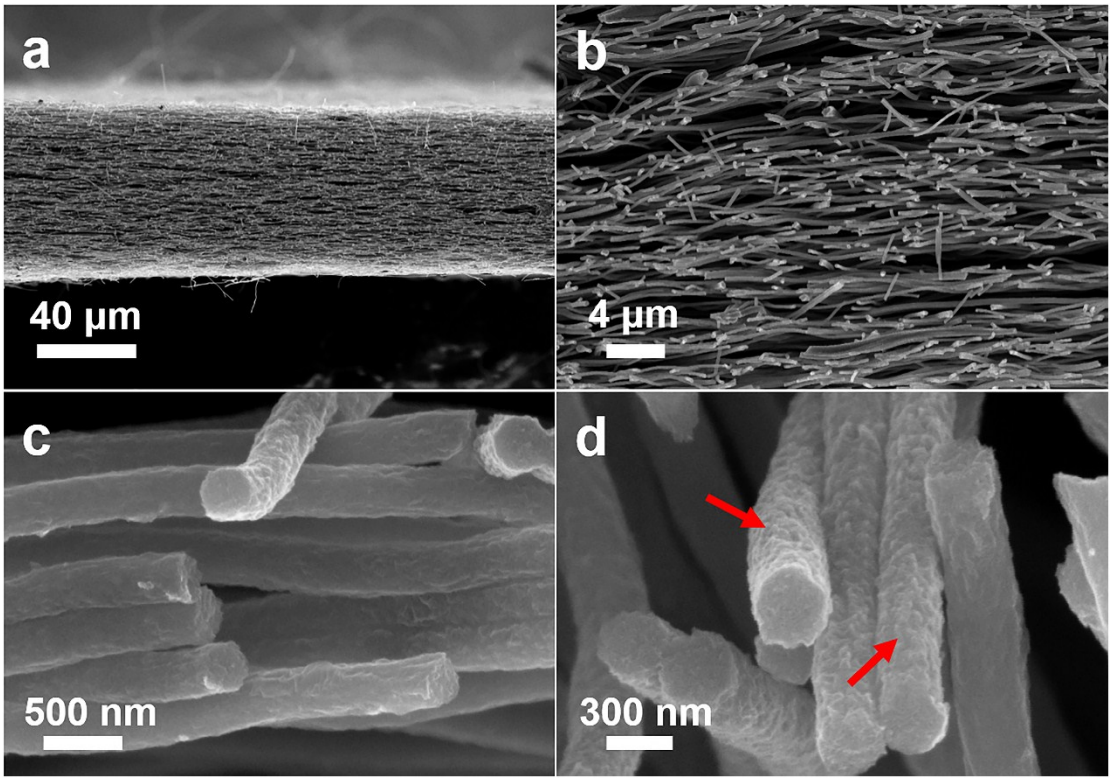

Fig. S2

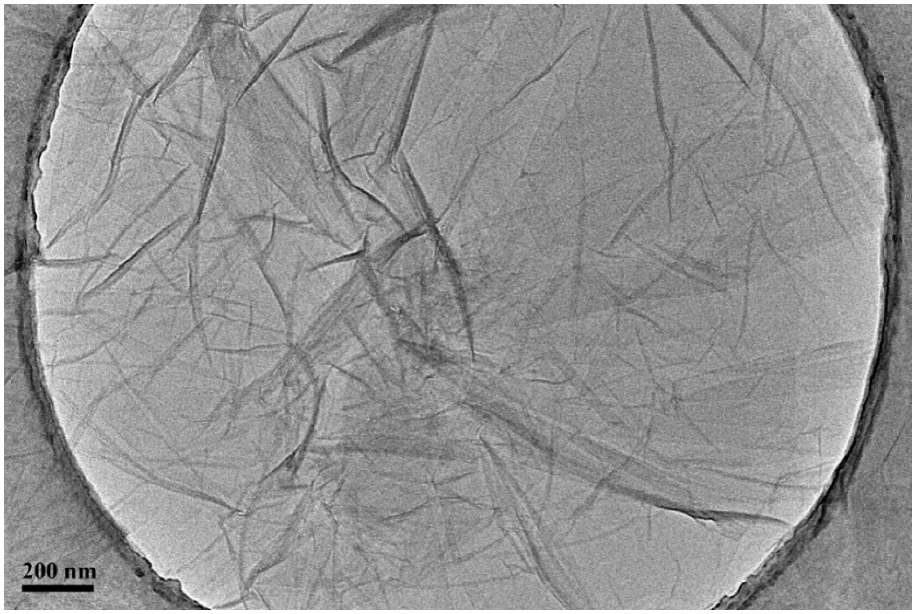

Fig. S3

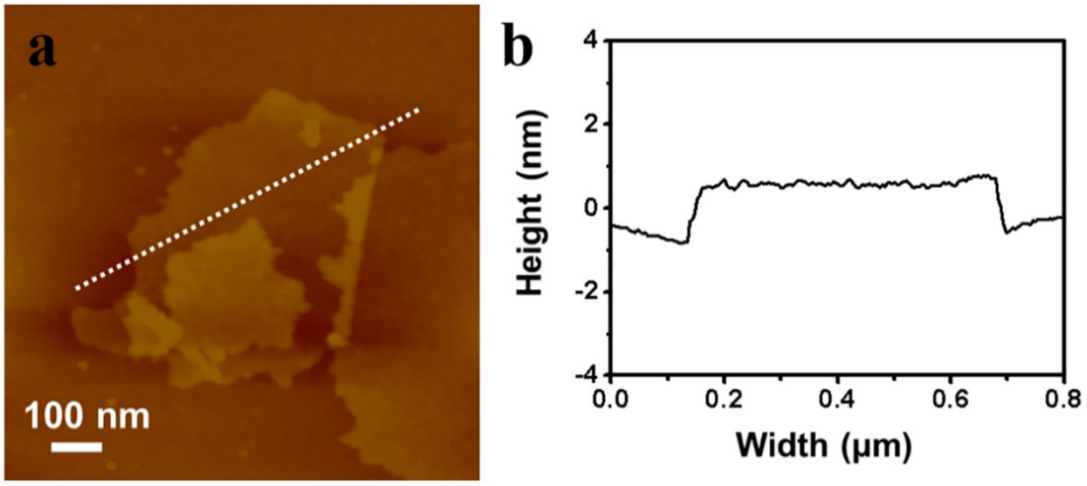

Fig. S4

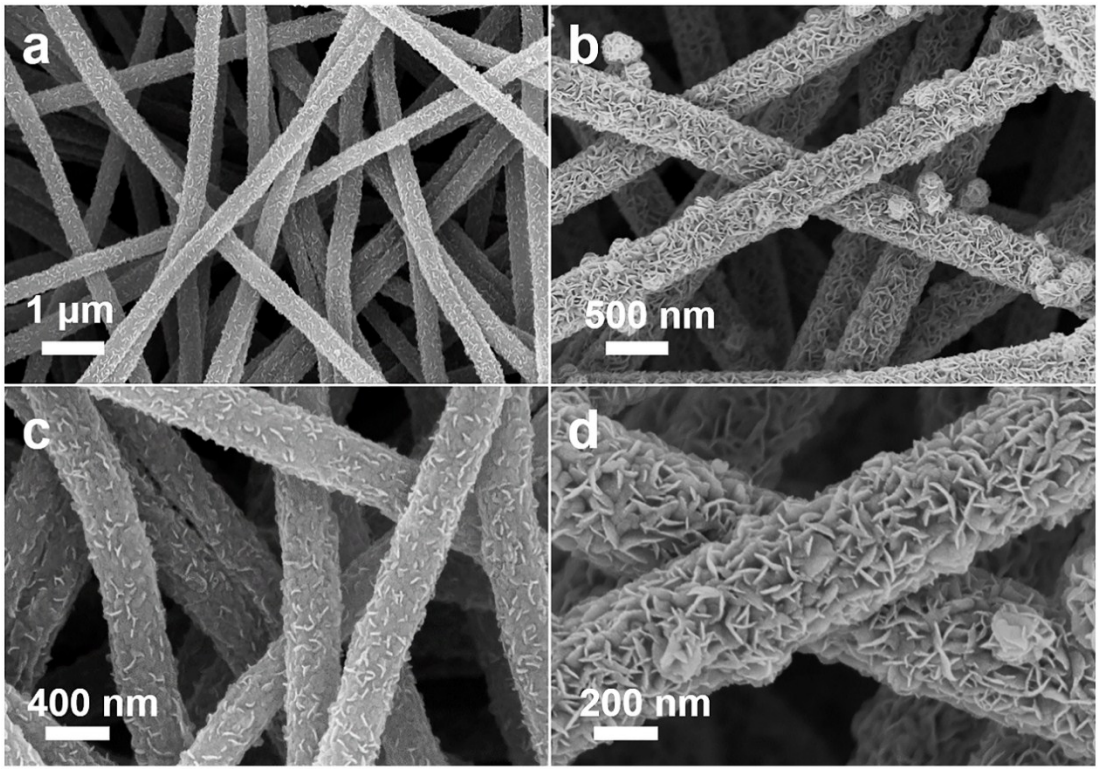

Fig. S5

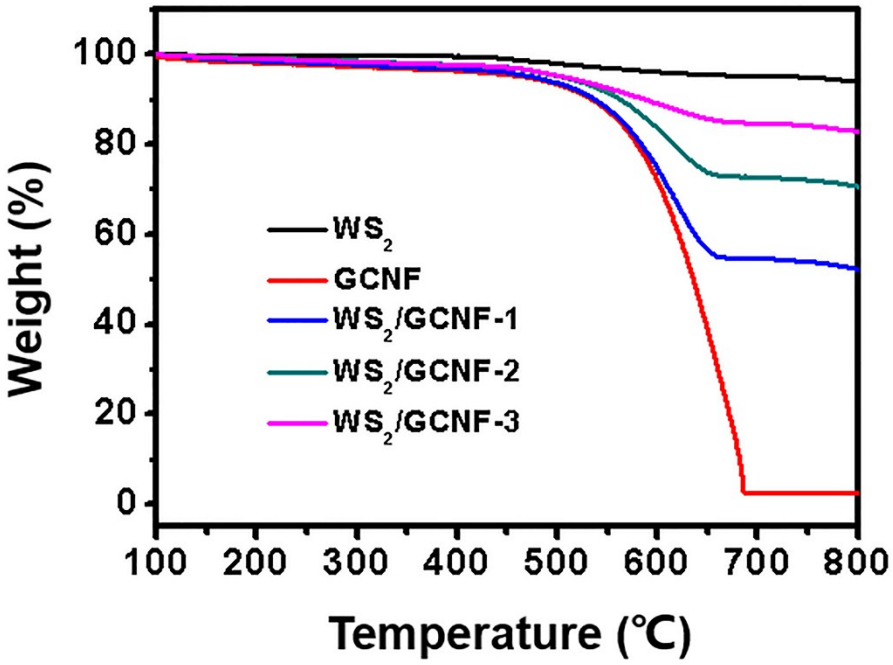
Weight (%)
100
80
60
40
20
0
100
200
300
400
500
600
700
800
Temperature (℃)
WS2
GCNF
WS2/GCNF-1
WS2/GCNF-2
WS2/GCNF-3

Fig. S6

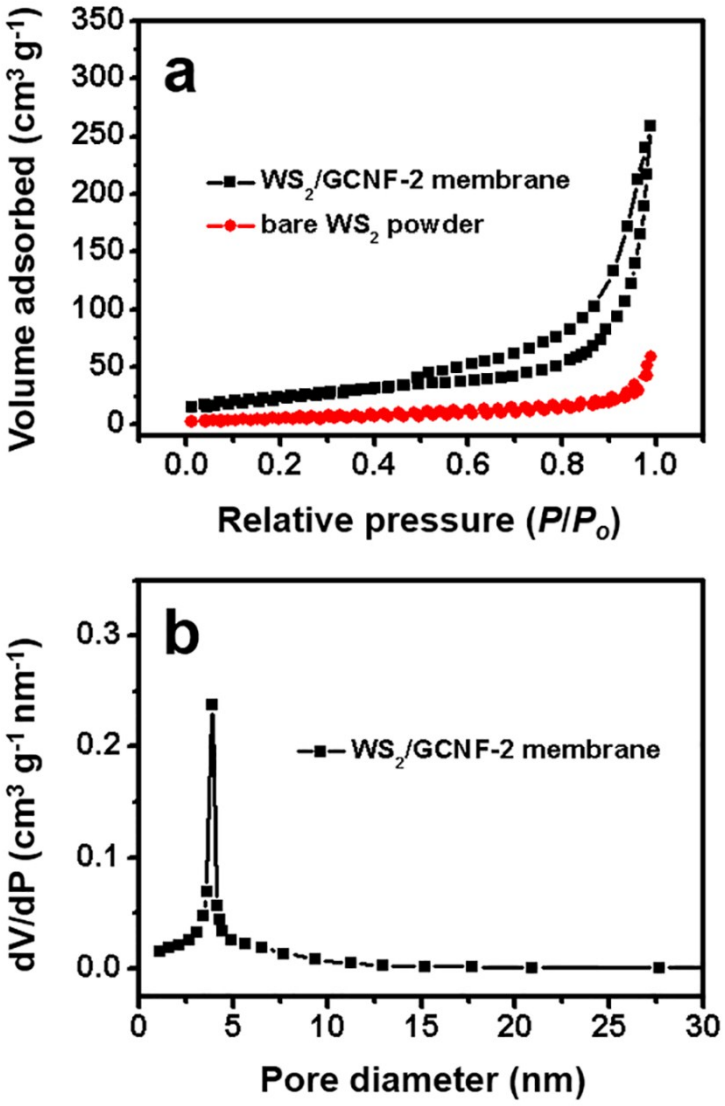
a
Volume adsorbed (cm3 g-1)
350
300
250
200
150
100
50
0
0.0
0.2
0.4
0.6
0.8
1.0
Relative pressure (P/Po)
WS2/GCNF-2 membrane
bare WS2 powder
b
dV/dP (cm3 g-1 nm-1)
0.3
0.2
0.1
0.0
0
5
10
15
20
25
30
Pore diameter (nm)
WS2/GCNF-2 membrane

Fig. S7

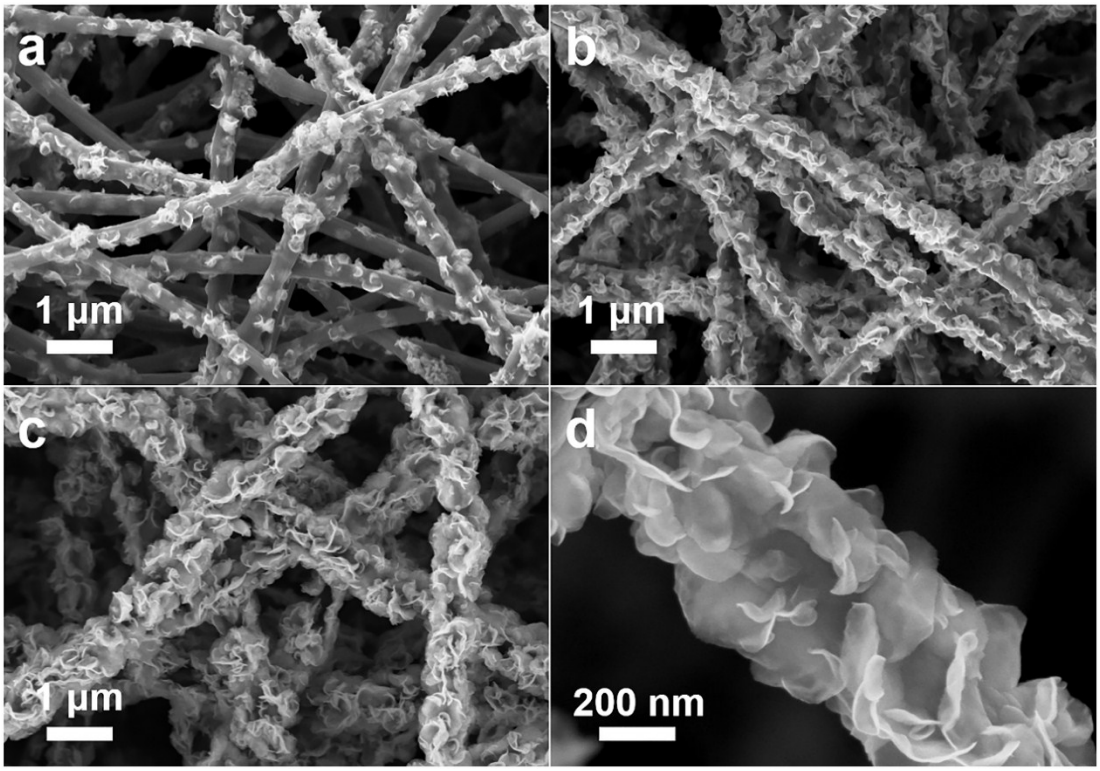

Fig. S8

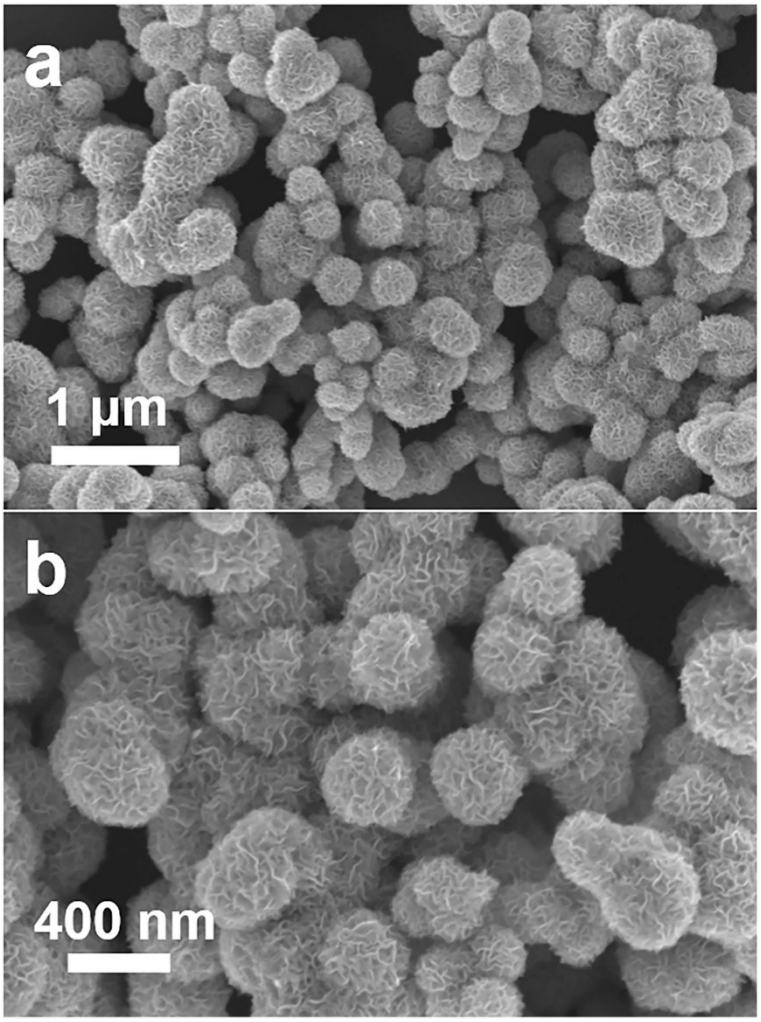

Fig. S9

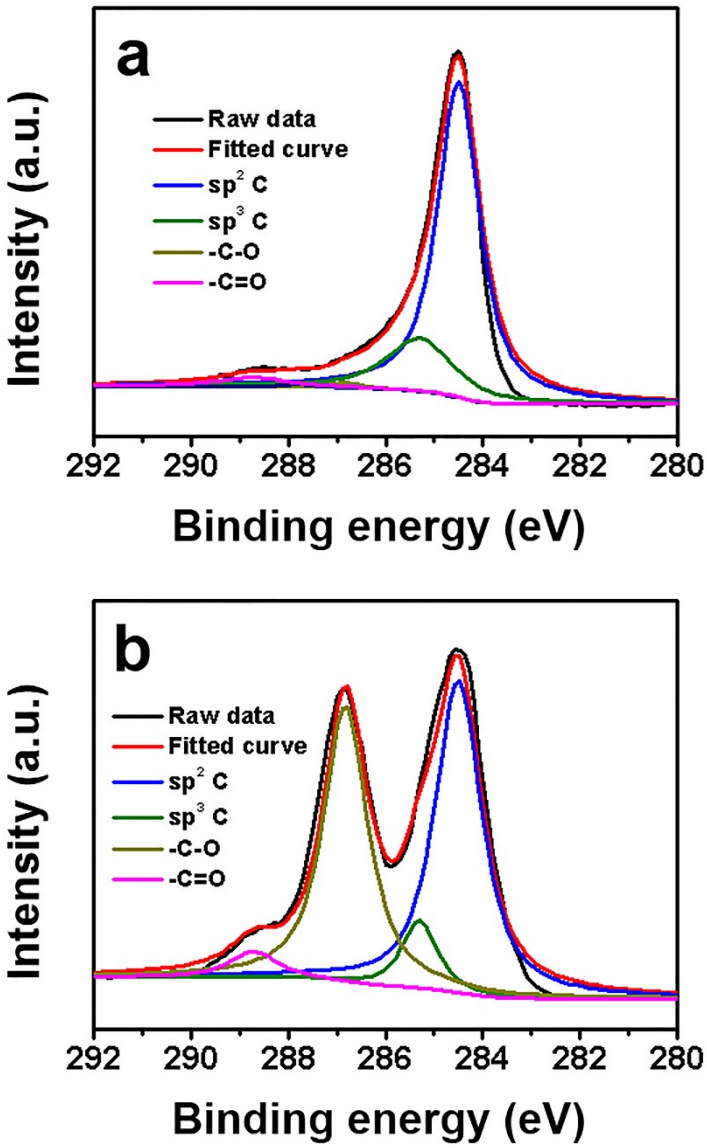
a
Raw data
Fitted curve
sp2 C
sp3 C
-C-O
-C=O
Intensity (a.u.)
292
290
288
286
284
282
280
Binding energy (eV)
b
Raw data
Fitted curve
sp2 C
sp3 C
-C-O
-C=O
Intensity (a.u.)
292
290
288
286
284
282
280
Binding energy (eV)

Fig. S10

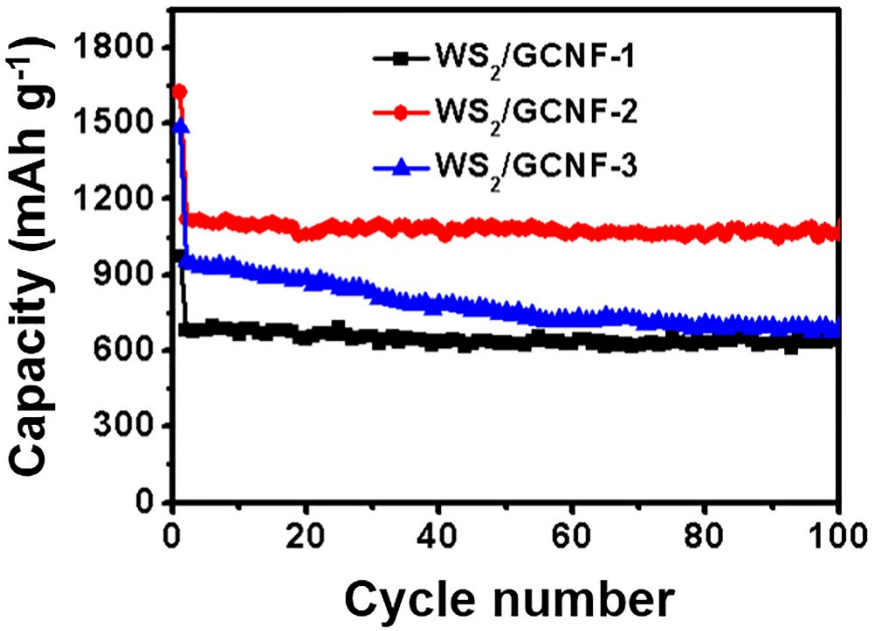
Capacity (mAh g-1)
1800
1500
1200
900
600
300
0
0
20
40
60
80
100
Cycle number
WS2/GCNF-1
WS2/GCNF-2
WS2/GCNF-3

Fig. S11

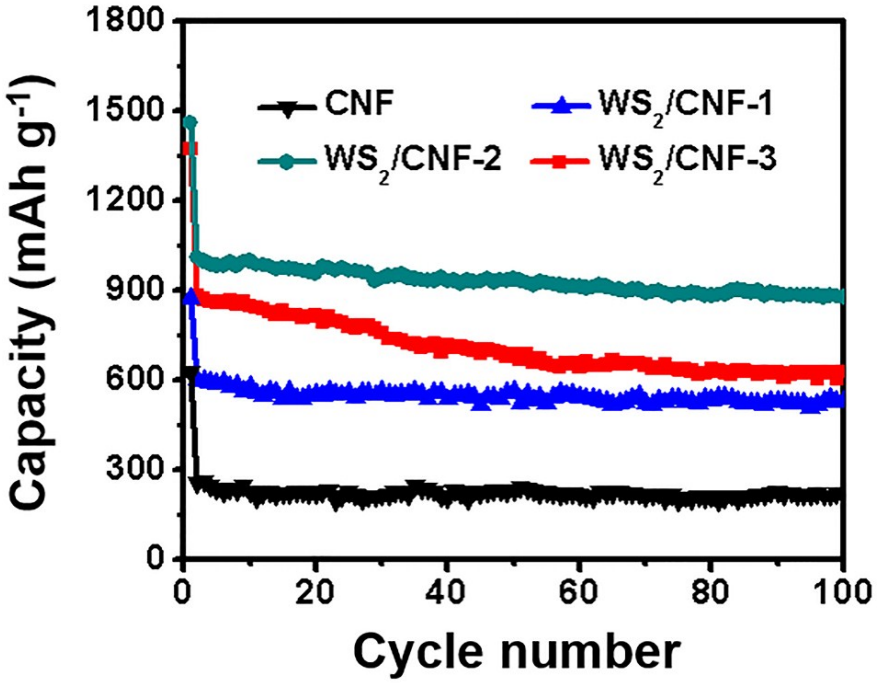
1800
1500
1200
900
600
300
0
Capacity (mAh g-1)
0
20
40
60
80
100
Cycle number
CNF
WS2/CNF-1
WS2/CNF-2
WS2/CNF-3

Fig. S12

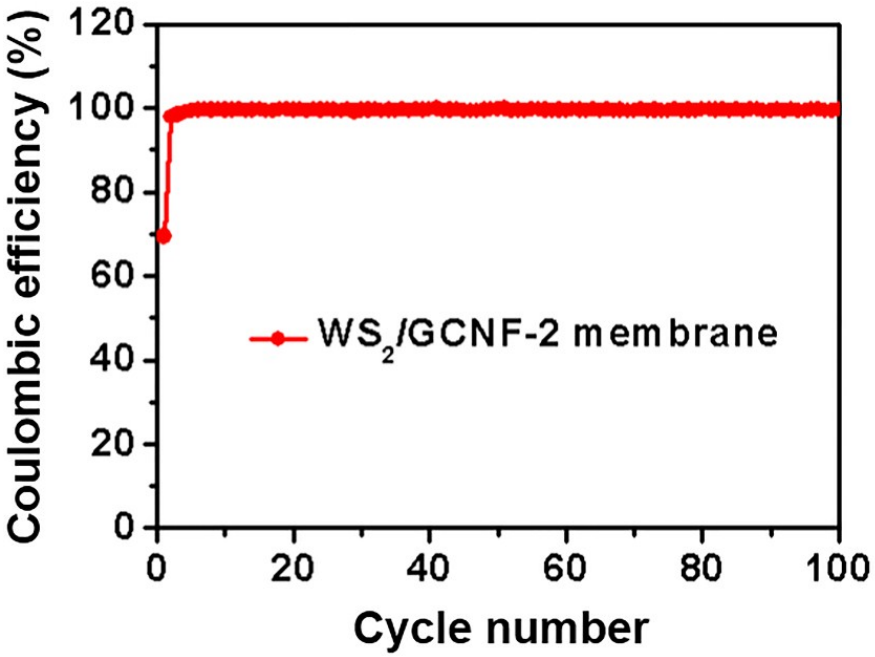
Coulombic efficiency (%)
120
100
80
60
40
20
0
0
20
40
60
80
100
Cycle number
WS2/GCNF-2 membrane

Fig. S13

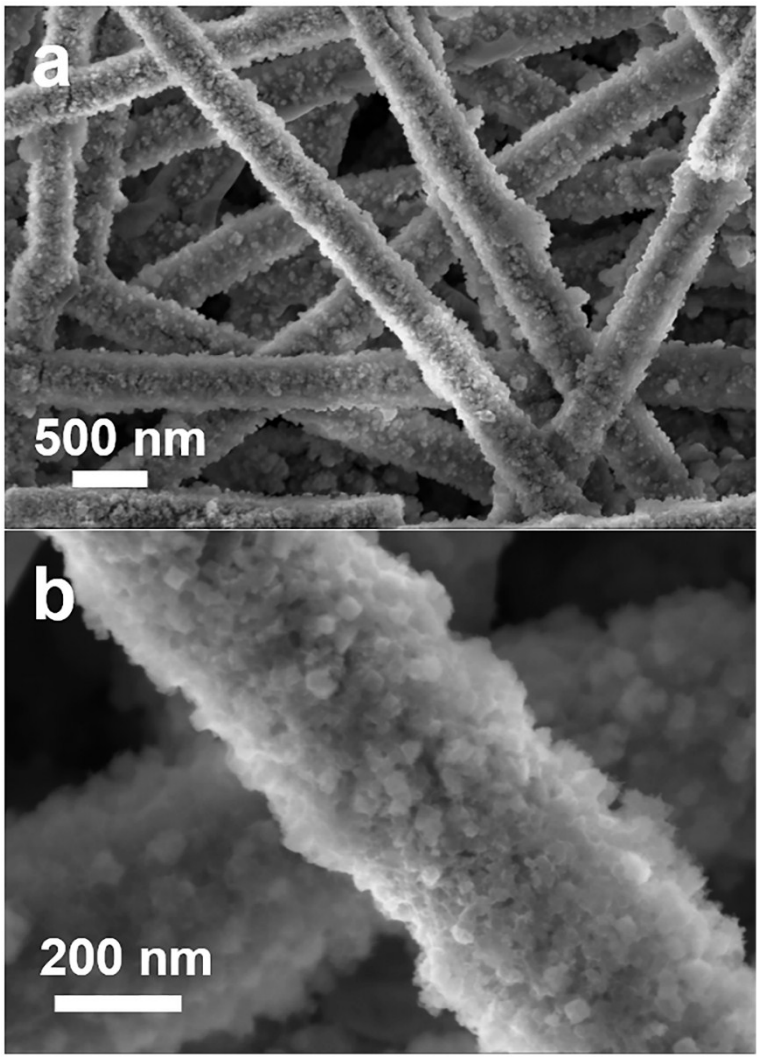

Fig. S14

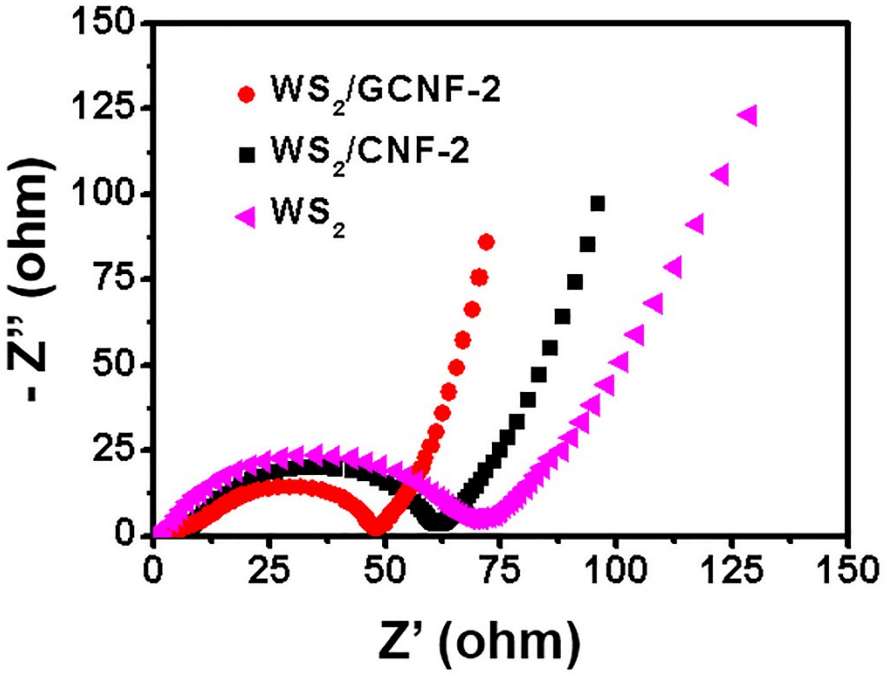
150
125
100
75
50
25
0
-Z'' (ohm)
0
25
50
75
100
125
150
Z' (ohm)
WS2/GCNF-2
WS2/CNF-2
WS2

Fig. S15